Nonparabolicity Effects in Quantum Cascade Lasers

G. Milovanovic and H. Kosina
Institute for Microelectronics
TU Wien
Gußhausstraße 27–29/E360, 1040 Wien, Austria
Email: milovanovic@iue.tuwien.ac.at

***Abstract*—We calculate electron-LO phonon and interface roughness scattering rates in a GaAs/Al_xGa_{1-x}As quantum cascade laser taking into account conduction subband nonparabolicity. In this work we investigate the Al concentration and the $\mathbf{k}_\parallel$ dependence of nonparabolicity effects. It is shown that the subband nonparabolicity may increase the electron-LO phonon scattering rates significantly, but the scattering rates are not qualitatively different from those in the parabolic approximation. Especially, we show that nonparabolicity leads to noticeable changes even for transitions involving electrons at the bottom of the subband and that this behaviour follows from the phonon wave vector and the electron phonon overlap.**

I. Introduction

Over the past several years, solid-state lasers based on intersubband transitions in semiconductor heterostructures have proved to be very promising candidates for practical sources of radiation, particularly in the midinfrared region [1]. While the possibility of optical amplification by intersubband transitions in biased superlattices had already been predicted in 1971 [2], a successfully working quantum cascade laser (QCL) has first been reported in 1994 [3].

Understanding the physics in these heterostructures is necessary to design and fabricate new QCL's with specific properties. In this work we adress the question how the subband nonparabolicity affects the electron-LO phonon scattering rates as well as the interface roughness scattering rates in a QCL subjected to barrier characteristics.

GaAs/Al_xGa_{1-x}As active regions grown on GaAs substrates are ideal candidates for this approach as Al_xGa_{1-x}As is nearly perfectly lattice matched to the GaAs substrate.

Frequently used theoretical models describing the electron properties in a semiconductor approximate the band structure by parabolic conduction bands. Deviations from the parabolic model are not considered in quantum well (QW) calculations based on effective mass approaches [4].

Here we investigate the influence of conduction band nonparabolicity on the intersubband scattering rates due to electron-LO phonon interactions and interface roughness, considering transitions with different initial energies. In order to determine for which situations the subband nonparabolicity can not be neglected, we show results of scattering rates for different $k_\parallel$ and make comparisons with the parabolic approximation. Our results demonstrate the significance of nonparabolicity effects in heterostructure lasers even for transitions where the initial state is at the bottom of the subband, particularly for scattering rates due to electron-LO phonon interaction, in situations of large electronic confinement. We identify the physical origins of the changes induced by conduction subband nonparabolicity in dependence on the Al content and the in-plane wave vector $\mathbf{k}_\parallel$ to be found in terms of the phonon wave vector and the electron phonon overlap.

In Sec. II we discuss the formal theory of the electron-LO phonon scattering rates, the interface roughness scattering model and the inclusion of the conduction band nonparabolicity in the effective mass equation. Our results are presented and discussed in Sec. III. Finally, a summary and conclusion is given in Sec. IV.

II. Theoretical Model

We consider electrons in the conduction band of a QCL in an electric field applied in the direction perpendicular to the heterointerfaces. In order to describe band nonparabolicity we follow the model proposed by Nag and Mukhopadhyay [5]. The nonparabolic $E-\mathbf{k}$ relation is given by

$$E - V(x) = \frac{\hbar^2 k^2}{2m^\star(x)}(1-\gamma(x)k^2) \tag{1}$$

where $\gamma(x)$ is the nonparabolicity parameter, $m^\star(x)$ is the effective mass, and $V(x)$ is the conduction band offset.

The envelope function in the QW structure is given by

$$\Psi_{i,k}(\mathbf{x}) = \frac{1}{\sqrt{A}} e^{i\mathbf{k}_\parallel\cdot\mathbf{x}_\parallel}\Phi_i(z) \tag{2}$$

where $\mathbf{k}_\parallel$ is the in-plane wave vector, A is the cross-sectional area of the QW structure, and $\Phi_i(z)$ is the electron envelope function of the ith state. The effective mass equation for the QW structure is given by

$$\left[-\frac{\hbar^2}{2}\frac{\partial}{\partial z}\frac{1}{m^\star_\perp(z,E)}\frac{\partial}{\partial z} + V(z) + \frac{\hbar^2 k_\parallel^2}{2m^\star_\parallel(z,E)} - eFz\right]\Phi_i(z) = E_i(k_\parallel)\Phi_i(z) \tag{3}$$

where the nonparabolic effective masses along the perpendicular and parallel directions are defined as [6]

$$m^\star_\perp(x,E) \equiv \frac{m^\star(x)}{\alpha(x)}[1-(1-2\alpha(x))^{1/2}] \tag{4}$$

$$m^\star_\parallel(x,E) \equiv \frac{m^\star(x)}{(1-2\alpha(x))^{1/2}} \tag{5}$$

978-1-4244-3927-0/09/$25.00 ©2009 IEEE

where $\alpha = 4\gamma(x)m^\star(x)(E - V(x))/\hbar^2$.
The Hamiltonian describing the electron-phonon interaction can be written in the form [7]

$$\hat{H}_{ep} = \sum_{i,j}\sum_{k,k'}\sum_{q}(F^{ij}_{k,k',q}c^\dagger_{i,k}b_q c_{j,k'} + F^{ij\star}_{k,k',q}c^\dagger_{j,k'}b^\dagger_q c_{i,k}) \quad (6)$$

with

$$\begin{aligned} F^{ij}_{k,k',q} &= F^{LO}_q \int \Psi^\star_{i,k}(\mathbf{x})e^{i\mathbf{q}\cdot\mathbf{x}}\Psi_{j,k'}(\mathbf{x})d\mathbf{x} \\ &= F^{LO}_q \delta_{\mathbf{k}'_\parallel,\mathbf{k}_\parallel-\mathbf{q}_\parallel}\int \Phi^\star_i(z)e^{iq_z z}\Phi_j(z)dz \quad (7)\end{aligned}$$

where $\mathbf{q}$ is the phonon wave vector, and $c^\dagger_{i,k}$ ($b^\dagger_q$) and $c_{i,k}$ (b_q) denote creation and annihilation operators of the electron (phonon), respectively. F^{LO}_q represents the coupling factor for the electron-LO phonon interaction

$$F^{LO}_q = -i\frac{e}{q}\left(\frac{\hbar\omega_{LO}}{2V\epsilon_0}(\epsilon^{-1}_\infty - \epsilon^{-1}_S)\right)^{1/2} \quad (8)$$

where ϵ_∞ and ϵ_S are high-frequency and static dielectric constants, V is the volume and e is the electronic charge.
The electron-LO phonon scattering rate for an electron initially in a state i to the final state j is obtained from the Fermi Golden Rule

$$W^\pm_{ij}(k_\parallel) = \frac{2\pi}{\hbar}\sum_{k'}|\langle j|\hat{H}_{ep}|i\rangle|^2\delta(E_j(k'_\parallel) - E_i(k_\parallel) \mp \hbar\omega_q) \quad (9)$$

by evaluating the matrix element in eq. (9) with the electron-phonon interaction Hamiltonian given by (6)

$$\begin{aligned} W^\pm_{ij}(k_\parallel) &= -\frac{2\pi}{\hbar}\sum_{k'_\parallel,q_z}\left[\frac{\hbar\omega_{LO}}{2V}(\epsilon^{-1}_\infty - \epsilon^{-1}_S)\right. \\ &\times\int\int\frac{e^2}{k'^2_\parallel + k^2_\parallel - 2k'_\parallel k_\parallel\cos\theta + q^2_z} \\ &\times\Phi^\star_i(z)e^{iq_z z}\Phi_j(z)d\theta dz\,(\frac{1}{2}\pm\frac{1}{2} + N_{LO}) \\ &\left.\times\delta(E_j(k'_\parallel) - E_i(k_\parallel) \mp \hbar\omega_q)\right] \quad (10)\end{aligned}$$

$\pm$ denoting emission and absorption processes, and N_{LO} is the phonon occupation number given by

$$N_{LO} = \frac{1}{e^{\hbar\omega_{LO}/k_BT} - 1} \quad (11)$$

The roughness of interfaces in a QW leads to spatial fluctuations in the width of the well, and consequently to fluctuations of the confinement energy. These fluctuations of the quantization energy act as a fluctuating potential for the motion of confined carriers [8].
The randomness of the interface is described by a correlation function at the in-plane position $\mathbf{r} = (x, y)$ which is usually taken to be Gaussian with a characteristic height of the roughness Δ, and a correlation length Λ representing a length scale for fluctuations of the roughness along the interface [9], such that

$$\langle\Delta(\mathbf{r})\Delta(\mathbf{r}')\rangle = \Delta^2 e^{-|\mathbf{r}-\mathbf{r}'|^2/\Lambda^2} \quad (12)$$

The perturbation in the potential $V(z)$ due to a position shift $\Delta(\mathbf{r})$ is given by

$$\delta V = V[z - \Delta(\mathbf{r})] - V(z) \approx -\Delta(\mathbf{r})\frac{dV(z)}{dz} \quad (13)$$

For the Ith interface, which is centered about the plane z_I and extends over the range $[z_{L,I}, z_{R,I}]$, the scattering matrix element can be defined as

$$\begin{aligned} M_{ji,I} &= \left\langle j\left|\delta V\,\mathrm{rect}(\frac{z - z_I}{z_{R,I} - z_{L,I}})\right|i\right\rangle \\ &= \frac{\varphi^2_{ji,I}}{A}\int\Delta(\mathbf{r})e^{i(\mathbf{k}_\parallel - \mathbf{k}'_\parallel)\cdot\mathbf{r}} \quad (14)\end{aligned}$$

where $|j\rangle$ and $|i\rangle$ denote the final and initial wave functions, respectively. $\varphi_{ji,I}$ is defined as

$$\varphi_{ji,I} = \int\Phi^\star_j(z)\frac{dV}{dz}\mathrm{rect}\left(\frac{z - z_I}{z_{R,I} - z_{L,I}}\right)\Phi_i(z)dz \quad (15)$$

and the rectangular function reads

$$\mathrm{rect}(z) = \begin{cases} 1, & |z| \le 0.5 \\ 0, & |z| > 0.5 \end{cases}$$

The expectation value of the square of the matrix element is given by

$$\langle|M_{ji,I}|^2\rangle = \frac{\varphi^2_{ji,I}}{A^2}\int\int\langle\Delta(\mathbf{r}')\Delta(\mathbf{r})\rangle e^{i(\mathbf{k}_\parallel - \mathbf{k}'_\parallel)\cdot(\mathbf{r}-\mathbf{r}')}d\mathbf{r}'d\mathbf{r} \quad (16)$$

Making use of eq. (12) and Fermi's Golden Rule, the interface roughness induced scattering rates are given by [10]

$$\begin{aligned} W^{IR}_{ij}(k_\parallel) &= \sum_I\frac{m^\star\Delta^2\Lambda^2\mid\varphi_{ji,I}\mid^2}{\hbar^3}\delta(E_{j,k'_\parallel} - E_{i,k_\parallel}) \\ &\times\int_0^\pi e^{-(\mathbf{k}'_\parallel - \mathbf{k}_\parallel)^2\Lambda^2/4}d\theta \quad (17)\end{aligned}$$

where $\mathbf{k}'_\parallel$ and $\mathbf{k}_\parallel$ are the final and initial wave vectors, respectively, and θ is the scattering angle.

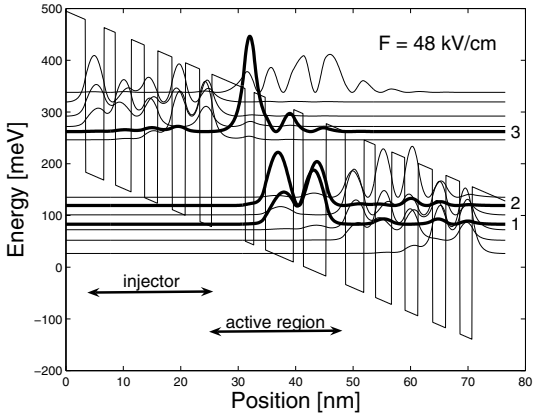

Fig. 1. A schematic diagram of the conduction band profile for one and a half periods of the GaAs/$Al_{0.3}Ga_{0.7}$As QCL for an electric field of 48 kV/cm. The layer sequence of one period, in nanometers, is: **3.4**, 3.2, **2**, 2.8, **2.3**, 2.3, **2.5**, 2.3, **2.5**, 2.1, **5.8**, 1.5, **2**, 4.9, **1.7** and 4, where normal scripts denote the wells and bold the barriers.

III. Results and Discussion

We consider a GaAs/$Al_xGa_{1-x}As$ QCL design which comprises a three-level sheme [11]. The conduction band profile for an electric field of 48 kV/cm is given in Figure 1.
The conduction band offset is determined as a function of the aluminum concentration x by the standard approximation [12]

$$\Delta E_c = \begin{cases} 0.75x\ eV, & x \in [0, 0.45] \\ 0.75x + 0.69(x - 0.45)^2\ eV, & x \in [0.45, 1] \end{cases}$$

The expression for the nonparabilicity parameters in terms of the energy gap were obtained from Ref. [13]

$$\gamma(x) = \frac{\hbar^2}{2m^\star(x)E_g(x)} \tag{18}$$

where the energy bandgap is $E_g(x) = (1.424 + 1.247x)m_0$ in the range $0 \leq x \leq 0.45$, and $E_g(x) = 1.900 + 0.125x + 0.143x^2$ for $x > 0.45$. The material parameters used in our calculations are for $Al_xGa_{1-x}As$ [14], the effective mass $m^\star(x) = 0.067 + 0.083x$, the dielectric constants $\epsilon_S = 13.18 - 3.12x$ and $\epsilon_\infty = 10.89 - 2.73x$, and the LO-phonon energies $\hbar\omega_{LO} = 36.25 - 6.55x + 1.79x^2$ meV. The characteristic height and the correlation length of the interface roughness are taken as $\Delta = 2.83$ Å and $\Lambda = 70$ Å.
In Figure 2 we show the calculated electron-LO phonon scattering rates for the intersubband transition $2 \rightarrow 1$ as a function of the Al content for $k_\parallel = 0$ nm^{-1}, $k_\parallel = 0.1$ nm^{-1} and $k_\parallel = 0.2$ nm^{-1}. The scattering rates with the inclusion of subband nonparabolicity are represented by solid lines and the dashed lines are for the parabolic band approximation. In general, the scattering rates are increased due to effects of nonparabolicity, except for intersubband transitions for large aluminum concentration, but the scattering rates are otherwise not qualitatively different from those in the parabolic band approximation. The variations of the electron-LO phonon scattering rates due to nonparabolicity are for transitions at the bottom of the subband of almost the same order as for transitions with higher initial energies. In the region of low Al concentration the nonparabolicity may cause a variation of about 8% for transitions initially at $k_\parallel = 0$ nm^{-1}, $\sim 10\%$ at $k_\parallel = 0.1$ nm^{-1} and $\sim 11\%$ at $k_\parallel = 0.2$ nm^{-1}. For larger aluminum content the effects due to subband nonparabolicity for transitions initially at the bottom of the subband are even higher than for initial conditions away from it.

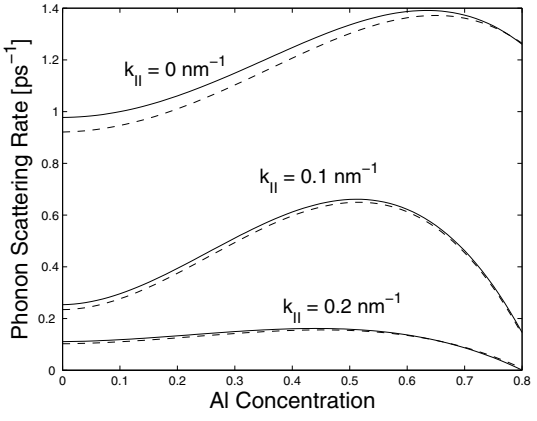

Fig. 2. Intersubband electron-LO phonon scattering rate for the transition $2 \rightarrow 1$ in a GaAs/$Al_xGa_{1-x}As$ structure as a function of the Al concentration x. Solid lines contain nonparabolicity and dashed lines are for parabolic bands.

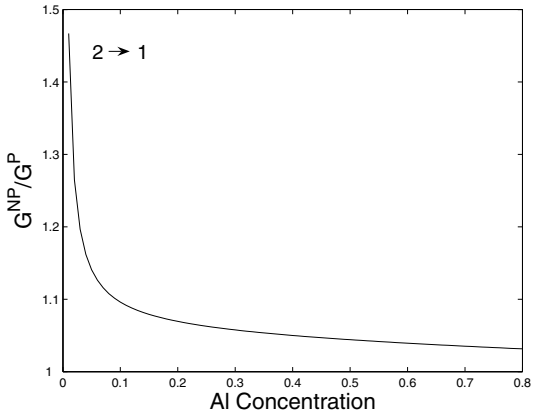

Fig. 3. Ratio of the nonparabolic and parabolic electron-phonon overlap integral as a function of aluminum content.

The nonparabolicity induced increase in the density of final states and of the quantum confinement, resulting in a larger electron-phonon overlap, and the influence of the subband on the phonon wave vector are mainly responsible for the variations in the transition rates. Since these variations are negligible for large x, the confinement decreases with the increase of the Al concentration and the effects of the nonparabolicity on the overlap integral become weaker. This is illustrated in Figure 3, where the ratio of the nonparabolic and parabolic electron-phonon overlap for the intersubband transition $2 \rightarrow 1$ is shown.
Since the electron-phonon interaction has a strong dependence on the phonon wave vector ($\propto 1/q$) it is crucial to investigate its behavior due to nonparabolicity in order to understand the influence of nonparabolic subbands on the electron-LO phonon scattering rates. Figure 4 shows that for nonparabolic subbands the phonon wave vector is larger than for parabolic subbands and that this effect becomes more pronounced for regions with higher in-plane wave vector of the electron $\mathbf{k}_\parallel$. Thus the electron couples more weakly to the phonon for nonparabolic subbands yielding a decrease of the electron-LO phonon scattering rates, which is more affected in case of larger phonon wave vectors. Although in situations of weak confinement the role of the phonon wave vector becomes more important, the decrease of scattering rates resulting from larger phonon wave vectors is compensated by the electron-phonon overlap integral. Hence these rates are generally larger for nonparabolic subbands. This explains why the variations in the electron-LO phonon scattering rates due to inclusion of nonparabolicity with higher initial electron in-plane vectors are of almost the same order as for $k_\parallel = 0$ nm^{-1} and in some situations of weak confinement even smaller.

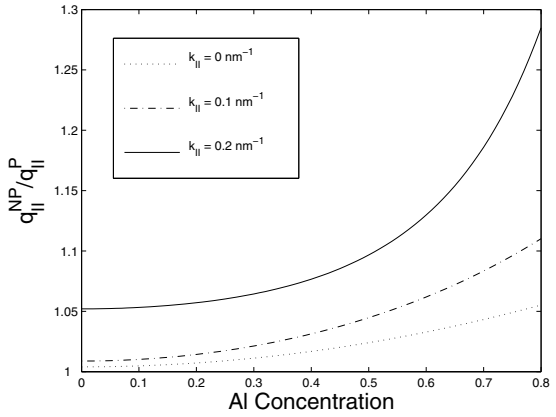

Fig. 4. Ratio of the averaged nonparabolic and parabolic phonon wave vector for the intersubband transition $2 \rightarrow 1$.

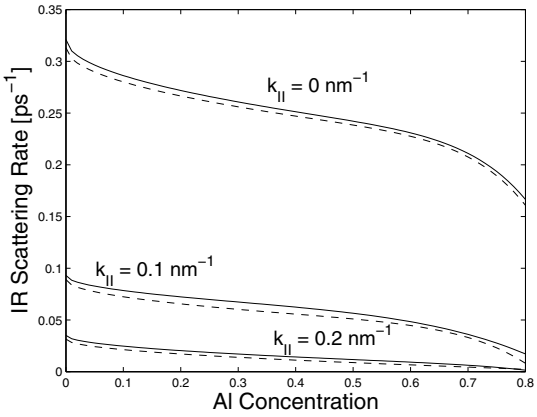

Fig. 5. Interface roughness induced scattering rate for the transition $2 \rightarrow 1$ as a function of the Al content in the barrier. Solid lines are transition rates with subband nonparabolicity and dashed lines are for parabolic bands.

The calculated scattering rates due to interface roughness as a function of Al concentration are illustrated in Figure 5. We show results for transitions where the initial state is at the bottom of the subband and away from it. In general, we observe that the variations on the interface roughness induced scattering rates due to nonparabolicity are approximately constant for all values of x. Numerically estimated we obtain variations of the order of 2-3 %. The effects of subband nonparabolicity on scattering rates due to electron-LO phonon interaction and interface roughness are better illustrated in Figure 6 where we display the ratio of the parabolic and nonparabolic scattering rates.

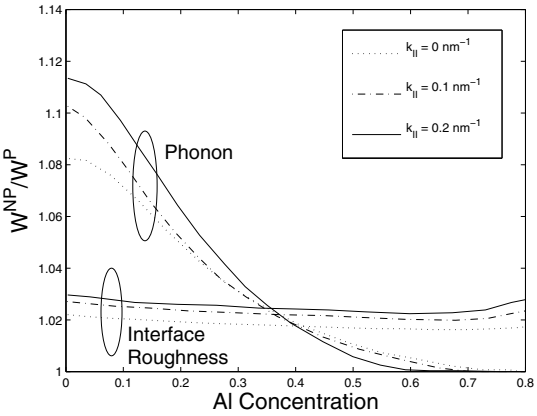

Fig. 6. Ratio of the nonparabolic and parabolic electron-LO phonon and interface roughness induced scattering rates as a function of the Al content.

IV. Conclusion

In conclusion, we have calculated the scattering rates of the intersubband transition $2 \rightarrow 1$ due to electron-LO phonon interaction and interface roughness in a GaAs/Al_xGa_xAs QCL at three different initial state conditions, namely at the bottom of the subband $k_{\|} = 0$ nm^{-1}, $k_{\|} = 0.1$ nm^{-1} and $k_{\|} = 0.2$ nm^{-1}. We find that the electron-LO phonon scattering rates are in general increased, except in situations of low confinement, which is equivalent to a large aluminum concentration. In particular, in situations of low aluminum concentration the results indicate the importance of including nonparabolicity in the conduction band due to a noticeable increase of the electron-LO phonon scattering rates even for transitions at the bottom of the subband, as the variations are of almost the same order as for initial states with larger electron in-plane vectors. We have shown that these subband nonparabolicity effects can be understood in terms of the electron-phonon overlap and the phonon wave vector.

Acknowledgment

This work has been supported by the Austrian Science Fund, special research program IR-ON (F2509).

References

[1] C. Gmachl, F. Capasso, D. L. Sivco, and A. Y. Cho, *Rep. Prog. Phys.*, **64**, 1533 (2001).
[2] R. F. Kazarinov, and R. A. Suris, *Sov. Phys. Semicond.*, **5**, 707 (1971).
[3] J. Faist, F. Capasso, D. L. Sivco, C. Sirtori, A. L. Hutchinson, and A. Y. Cho, *Science*, **264**, 553 (1994).
[4] N. Schildermans, M. Hayne, V. V. Moshchalkov, A. Rastelli, and O. G. Schmidt, *Phys. Rev. B*, **72**, 115312 (2005).
[5] B. R. Nag, and S. Mukhopadhyay, *Phys. Status Solidi B*, **175**, 103 (1993).
[6] S. Panda, and B. K. Panda, *J. Appl. Phys.*, **101**, 043705 (2007).
[7] T. Kuhn, and F. Rossi, *Rev. Mod. Phys.*, **74**, 895 (2002).
[8] U. Penner, H. Rücker, and I. N. Yassievich, *Semicond. Sci. Technol.*, **13**, 709 (1998).
[9] S. Tsujino, A. Borak, E. Müller, M. Scheinert, C. V. Falub, H. Sigg, D. Grützmacher, M. Giovannini, and J. Faist, *Appl. Phys. Lett.*, **86**, 062113 (2005).
[10] T. Unuma, M. Yoshita, T. Noda, H. Sakaki, and H. Akiyama, *J. Appl. Phys.*, **93**, 1586 (2003).
[11] C. Sirtori, P. Kruck, S. Barbieri, P. Collot, J. Nagle, M. Beck, J. Faist, and U. Oesterle, *Appl. Phys. Lett.*, **73**, 3486 (1998).
[12] P. J. Turley, and S. W. Teitsworth, *Phys. Rev. B*, **44**, 3199 (1991).
[13] D. F. Nelson, R. C. Miller, and D. A. .Kleinman, *Phys. Rev. B*, **35**, 7770 (1987).
[14] S. Adachi, *J. Appl. Phys.*, **58**, R1 (1985).